The QSO proximity effect: evidence for overdensity around quasars at $2 < z_{em} < 3$

M.Bruscoli[1,2], V.D'Odorico[3], F.Saitta[1,4], S.Cristiani[3], F.Fontanot[5], P.Monaco[1] & M.Viel[3]

1Dip. di Astronomia, Università di Trieste, Italy; 2 IRA-INAF, Firenze, Italy; 3 INAF-OATS, Trieste, Italy; 4 ESO, Garching bei Munchen, Germany; 5 Max-Planck-Institute for Astronomy, Heidelberg, Germany

INTRODUCTION: The absorption lines seen blueward of the HI Lyα emission line in spectra of QSOs at high redshifts are attributed to neutral hydrogen (HI) tracing the low to intermediate-density baryon distribution along the line of sight. The observations show that the number density of Lyα lines increases with redshift, but within single quasar spectra the number density of Lyα lines decreases as the redshift approaches the quasar emission redshift (z_{em}). This effect was first discovered by Carswell et al. (1982, MNRAS, 198, 91) and confirmed by later studies (e.g. Tytler 1987, ApJ, 321, 69). Bajtlik et al. (1988, ApJ, 327, 570) called this deficiency of Lyα absorptions near the background quasar *proximity effect* and attributed it to the increased ionization of Lyα clouds near the QSOs due to their ionizing flux.

From these studies on, the proximity effect has been used to estimate the intensity J_ν of the ultraviolet background radiation (UVB) (Bechtold 1994, ApJS, 91, 1; Giallongo et al. 1996, ApJ, 466, 46; Scott et al. 2000, ApJS, 130, 67) and more recently to explore the distribution of matter near the QSOs (Guimaraes et al. astro-ph/0702369v1).

Tab.1 shows some results for J_ν taken from the literature.

DATA SAMPLE: We have used the high quality spectra of 18 QSOs observed with UVES at the ESO VLT at a resolution R~ 45000 and typical S/N~60-100 per pixel (ESO Large Program 'The cosmic evolution of the IGM'). The wavelength range goes from 300 to 1000 nm. To this sample we added the spectrum of the QSO J2233-606 observed at the same resolution and S/N~30-40 per pixel. For the determination of the QSO systemic redshift, critical in this kind of analysis, we made averages of the redshifts of all the emission lines we detected in our spectra corrected by the factors computed by Tytler & Fan (1992, ApJ Suppl. S. 79,1) to take into account the systematic velocity shifts affecting the UV emission lines. The main characteristic of the QSOs forming our sample are reported in Tab.2.

$J_{\nu LL} \times 10^{-21}$	Γ_{12}	reference
1	2.64	Bajtlik et al. 1988
3	7.91	Bechtold 1994
0.5	1.32	Giallongo et al. 1996
1.4	3.69	Scott et al. 2000
0.7	1.85	Scott et al. 2000

Tab1: $J_{\nu LL}$ is the intensity of the UVB at the Lyman limit in ergs cm^{-2} s^{-1}Hz^{-1}sr^{-1}. The redshifts range of the used observations is approximately 1.6 < z < 4.1.
From $J_{\nu LL}$ we recover the hydrogen photoionization rate Γ_{12} through the approximated relation: $J_{\nu LL} = 0.079\ (\alpha + 3)\ \Gamma_{12} \times 10^{-21}$ with α=1.8.

QSO	z_{em}	Δ_z	$\Gamma_\nu \times 10^{40} [s^{-1} cm^2]$	$r_{QSO} [Mpc]$
HE1341-1020	2.139	1.648-2.139	0.10973	2.998
Q0122-380*	2.203	1.702-2.203	0.77395	7.362
PKS1448-232*	2.220	1.716-2.220	1.0358	8.177
PKS0237-23*	2.233	1.728-2.233	1.2824	9.471
J2233-606	2.250	1.742-2.250	1.3627	9.025
HE0001-2340	2.267	1.756-2.267	1.1814	8.988
Q0109-3518	2.407	1.874-2.407	1.7484	10.035
HE2217-2818	2.415	1.881-2.415	2.3691	12.230
Q0329-385*	2.440	1.902-2.440	1.5631	9.638
HE1158-1843	2.451	1.911-2.451	1.2448	8.870
HE1347-2457	2.560	2.003-2.560	0.66469	7.532
Q0453-423	2.662	2.089-2.662	0.64660	7.107
PKS0329-255	2.698	2.120-2.698	0.78574	6.810
HE0151-4326	2.761	2.173-2.761	1.6643	10.249
Q0002-422	2.768	2.179-2.768	1.4090	9.609
HE2347-4342	2.878	2.272-2.878	2.3729	11.446
HE0940-1050	3.088	2.449-3.088	2.5290	14.507
Q0420-388	3.123	2.478-3.123	2.5594	12.369
PKS2126-158	3.275	2.607-3.275	3.4059	13.784

Tab2: z_{em} is the emissione redshift; $\Delta z = z_{LyB} - z_{em}$ is the redshifts interval used for each quasar; Γ_ν is the quasar photoionization flux; r_{QSO} is the radius of the influence zone of each quasar (in proper Mpc).

COSMOLOGICAL SIMULATIONS: We used simulations run with the parallel hydrodynamical (TreeSPH) code GADGET-2 (Springel 2005, MNRAS, 364, 1105). They consist of a cosmological volume with periodic boundary conditions filled with 2×400^3 dark matter and gas particles. Having a large box, 120h^{-1} comoving Mpc, is crucial since the influence zone of the QSOs is usually of the order of some or tens of proper Mpc. We analysed the output at z=2.2: we traced about 200 lines of sight intersecting the center of the 200 most massive haloes that should host the QSOs ($M>10^{12} M_{SUN}/h$). More details can be found in Viel et al. (2004, MNRAS, 354, 684).

A NEW STATISTICAL INDICATOR: In previous works, authors derived the proximity effect from the number density of the Lyα absorption lines obtained from their QSOs sample: this number depends on how the Voigt profile fitting is executed. Problems arise principally in the fitting analysis of the complex absorption lines where the decomposition in Voigt profiles is not univocally determined. In this work we adopt a new method based on the fact that the sum of the neutral hydrogen column density (NHI) of the velocity components in the complex absorption lines is conserved indipendently of the number of Voigt profiles used for the decomposition.

We therefore convert the observed NHI, in the optical thin approximation (NHI<10^{17} cm^{-2}), in observed hydrogen number density n_H and then we compare the observed density contrast ($\delta+1=n_H/\langle n_H\rangle$) with the synthetic density contrast obtained from the adopted cosmological simulations. The study of the two density contrasts behaviours as a function of the QSOs distance, allow us to draw important conclusions on the mutual interplay of clustering and QSOs ionizing flux in giving origin to the proximity effect. As direct consequence, we infer a realistic limit on the $J_{\nu LL}$ estimate.

To convert the observed NHI in n_H we use the approximation given in Schaye (2001, ApJ, 559,507):

$$NHI \sim 2.3\times10^{13}\,cm^{-2}\,(n_H/10^{-5}\,cm^{-3})^{3/2}\,T_4^{-0.26}\,\Gamma_{12}^{-1}\,(f_g/0.16)^{1/2} \qquad (1)$$

where $T_{IGM}=T_4\times10^4$ K is the IGM temperature, $\Gamma=\Gamma_{12}\times10^{-12}$ s^{-1} is the hydrogen photoioniztion rate and $f_g \sim \Omega_b/\Omega_m$ is the fraction of mass in gas (stars and molecules are not included).

We choose as fiducial values: T_{IGM}=18000 K (the temperature at the mean density measured in the simulations), $\Gamma_{12}=1$ as recent studies and simulations suggest at 2< z <4.

To apply this approximation, the lists of observed Lyα lines have been converted into lists of Lyα absorbers with radius of the order of the local Jeans length.

THE PROXIMITY EFFECT: All the data of the 19 QSOs sample are then analyzed together: in each bin of 5 proper Mpc, ranging from the quasar (r=0) to the extension of the simulations box (r= 52 proper Mpc), we take the median of all the values of the density contrast fallen inside the bin. As a first approximation we computed the proximity effect using only the UVB as ionizing flux in Eq.1 and so $\Gamma_{12}=\Gamma_{UVB}/10^{-12}$ s^{-1}, then we have introduced in Eq.1 the contribution, for each quasar, of its ionizing flux and the total ionizing radiation is now $\Gamma_{12}=\Gamma_{UVB}(1+\Gamma_{QSO}/\Gamma_{UVB})/10^{-12}$ s^{-1} (Fig.1). We investigate also the following effects on the proximity effect: *i)* the variation of T_{IGM} (Fig.2); *ii)* the variation of Γ_{12} (Fig.3).

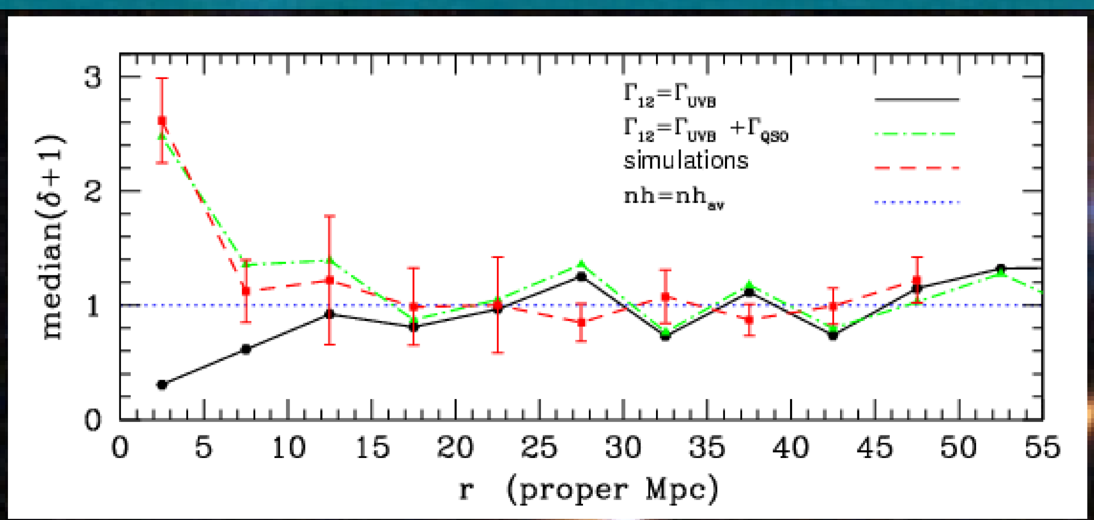

FIG1: comparison between the proximity effect derived from simulations (dashed line) and the proximity effect for the 19 QSOs sample: Γ_{UVB} only (solid line) and $\Gamma_{UVB}+\Gamma_{QSO}$ (dashed-dotted line). The dotted line gives the mean overdensity.

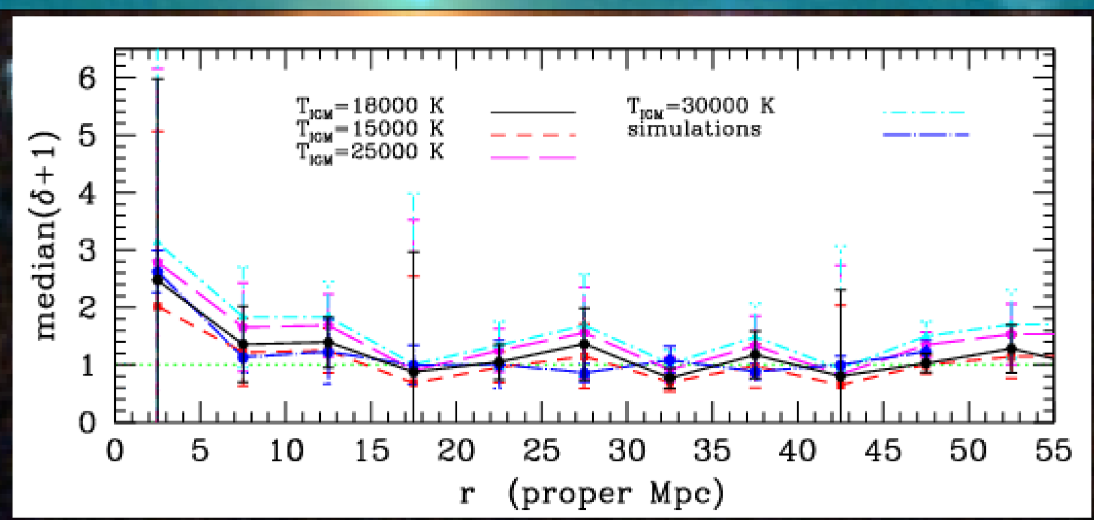

FIG2: comparison between the proximity effect obtained from simulations and the proximity effect derived assuming different values of the mean IGM temperature between 15000 and 30000 K.

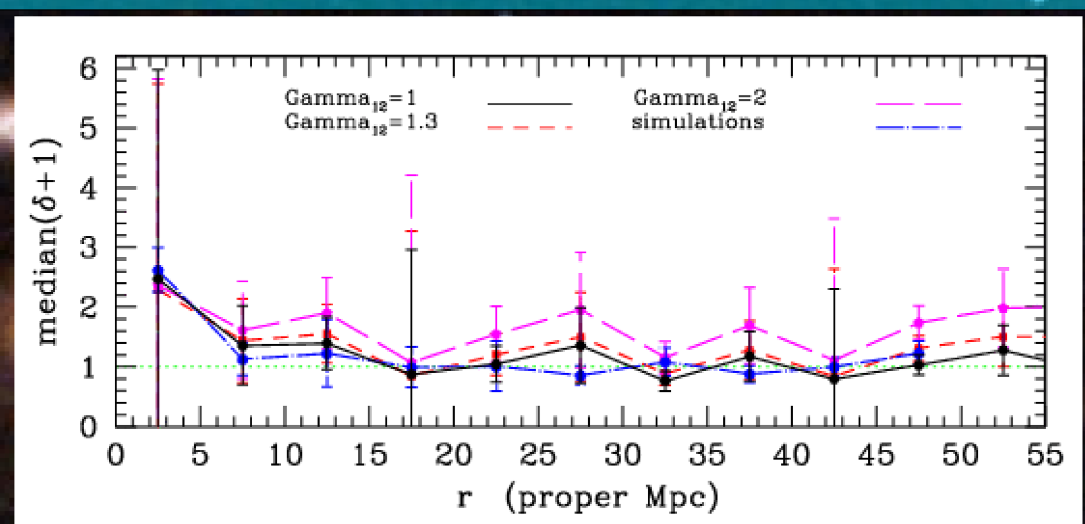

FIG3: comparison between the simulations proximity effect and the proximity effect obtained varying the photoionization rate Γ_{12} in the range 1-2, in agreement with studies on the IGM opacity (Bolton et al. 2005, MNRAS, 357, 1178).

CONCLUSIONS: The introduction of Γ_{QSO}, reproducing the behaviour of the simulations proximity effect that take into account the fact that each quasar lies in a overdensity peak, supports the idea that QSOs reside in overdense regions respect to the mean IGM. The comparison with cosmological simulations in the mean IGM, shows that values of Γ_{12} > 2 can be ruled out and that T_{IGM} should be in the range 15000-20000 K. We are not able to put a more robust limit on Γ_{12} due to the error bars: more high resolution QSOs spectra are required to reduce the uncertainties.